

# Meteosat Second Generation Cloud Algorithms for Use at AFWA

Stanley Q. Kidder<sup>\*</sup>, J. Adam Kankiewicz, and Kenneth E. Eis  
*DoD Center for Geosciences / Atmospheric Research*  
*Colorado State University*  
*Fort Collins, Colorado*

## ABSTRACT

The first of the second generation of Meteosats (Meteosat 8) became operational on 29 January 2004. Whereas previous operational satellites had two channels (DMSP/OLS), three channels (Meteosats 1–7), or five channels (NOAA/AVHRR, GOES Imager), Meteosat 8, with eleven 3-km resolution channels, offers many opportunities to improve cloud detection and characterization to aid military planners. In this paper, we outline six Meteosat 8 algorithms which we have developed for implementation at AFWA. These algorithms are Cloud Mask, Nocturnal Cloud Mask, Daytime Cirrus, Nocturnal Thin Cirrus, Precipitating Clouds, and Multi-Channel Skin Temperature.

## 1. INTRODUCTION

Meteosat Second Generation (MSG) represents a major advance in observing capability from previous operational meteorological satellites. The first of these satellites, Meteosat 8, become operational on 29 January 2004. The Spinning Enhanced Visible and Infrared Imager (SEVIRI), with eleven 3-km-resolution channels and one 1-km-resolution visible channel (Table 1), offers many opportunities to improve on cloud detection and characterization algorithms which are now used with data from the five-channel GOES Imager (the first of which became operational on 1 November 1994), from the five-channel (now six-channel) Advanced Very High Resolution Radiometer (AVHRR, first launched in 1978), or from the two-channel Operational Linescan System (OLS, first launched in 1976). Wanting to exploit the new information in these MSG data, AFWA contracted the Center for Geosciences/Atmospheric Research (CG/AR) through Lockheed Martin to develop algorithms based on the CG/AR's prior 6.2 research. The products described in this paper will also be created from data from the Advanced Baseline Imager (ABI), which will be launched on the next generation of GOES satellites (in approximately 2012).

**Table 1.** MSG SEVIRI Channels

Band	Center ( $\mu\text{m}$ )	99% Energy Band ( $\mu\text{m}$ )	Resolution (km)	Band	Center ( $\mu\text{m}$ )	99% Energy Band ( $\mu\text{m}$ )	Resolution (km)
HRV	0.75		1	IR 10.8	10.8	9.80 - 11.80	3
VIS 0.6	0.635	0.56 - 0.71	3	IR 12.0	12.0	11.00 - 13.00	3
VIS 0.8	0.81	0.74 - 0.88	3	WV 6.2	6.25	5.35 - 7.15	3
IR 1.6	1.64	1.50 - 1.78	3	WV 7.3	7.35	6.85 - 7.85	3
IR 3.9	3.92	3.48 - 4.36	3	IR 9.7	9.66	9.38 - 9.94	3
IR 8.7	8.70	8.30 - 9.10	3	IR 13.4	13.40	12.40 - 14.40	3

<sup>\*</sup> Corresponding author address: Dr. Stanley Q. Kidder, CIRA/Colorado State University, 1375 Campus Delivery, Fort Collins CO 80523-1375, (970) 491-8367, Stanley.Kidder@ColoState.edu.

## 2. ALGORITHMS

Six algorithms were developed for AFWA, most with the idea that wavelengths not currently in use should be exploited. The six algorithms are named Cloud Mask, Nocturnal Cloud Mask, Daytime Cirrus, Nocturnal Thin Cirrus, Precipitating Clouds, and Multi-Channel Skin Temperature. They are discussed in the next six sections.

### 2.1. Cloud Mask

Most cloud algorithms start with a cloud mask, which determines whether a pixel is cloudy or not. If the pixel is determined to be cloudy, properties of the cloud are then retrieved.

For the MSG cloud mask, we chose to use a difference-from-background technique similar to that used in the International Satellite Cloud Climatology Project (ISCCP, Schiffer and Rossow 1983). The process starts by constructing a 10-day infrared background (IRB) for each hour of the day. We chose to use the 8.7  $\mu\text{m}$  channel rather than the traditional 10.8  $\mu\text{m}$  channel because it seemed to perform better over land, perhaps due to slightly less water vapor absorption. The IRB is the 8.7  $\mu\text{m}$  radiance at each pixel location for each hour observed during the previous ten days. The data base is updated every hour. Thus, for each pixel the database contains 240 entries (10 days times 24 hours). When new data are processed, the database is updated by removing the oldest values and adding the newest values. This process assumes that there is no change in the image-to-image navigation of the Meteosat-8 data. It also assumes that in 10 days each pixel is observed to be cloud-free at least once.

The infrared background cloud test exploits the tendency of clouds to be colder than the underlying surface. Pixels whose radiance is less than the background radiance by more than a threshold value are flagged as cloudy. Over water the threshold is  $7.5 \text{ W m}^{-2} \text{ sr}^{-1} \mu\text{m}^{-1}$ ; over land it is  $30 \text{ W m}^{-2} \text{ sr}^{-1} \mu\text{m}^{-1}$ . Figure 1 shows an example.

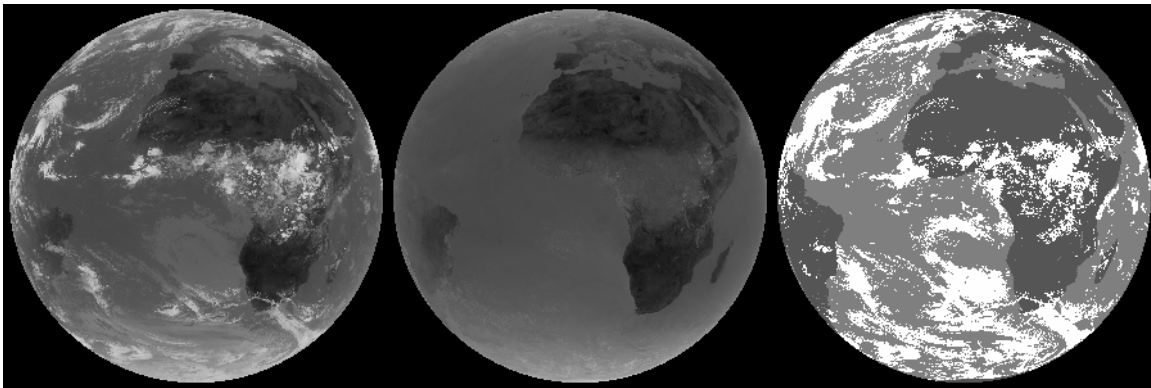


**Figure 1.**  $T_{8.7}$  (left); 10-day background at 1215 UTC (center); cloud mask (right).

### 2.2. Nocturnal Cloud Mask

The nocturnal cloud mask test uses the brightness temperature at 10.8  $\mu\text{m}$  and the albedo at 3.9  $\mu\text{m}$  (determined from the measured 3.9 and 10.8  $\mu\text{m}$  radiances) to detect ice clouds, liquid water clouds, and clear scenes (Kidder et al. 2000). 8.7  $\mu\text{m}$  data are used to screen desert pixels.

At night the 3.9  $\mu\text{m}$  albedo is calculated as

$$A_{3.9} = \frac{B_{3.9}(T_{10.8}) - L_{3.9}}{B_{3.9}(T_{10.8})}, \quad (1)$$

Where  $L_{3.9}$  is the satellite-observed radiance at 3.9  $\mu\text{m}$ ,  $T_{10.8}$  is the satellite measured brightness temperature at 10.8  $\mu\text{m}$ , and  $B_{\lambda}(T)$  is the Planck function. Liquid water clouds have a 3.9  $\mu\text{m}$  albedo approaching 0.3, and cirrus clouds (being mostly thin) have a negative 3.9  $\mu\text{m}$  albedo due to leakage of radiation through the cloud. Ocean, snow cover and most land have a near-zero 3.9  $\mu\text{m}$  albedo. Some desert scenes have a high 3.9  $\mu\text{m}$  albedo which must be screened. In this screening process, it is convenient to apply Eq. 1 to the 8.7  $\mu\text{m}$  data:

$$A_{8.7} \equiv \frac{B_{8.7}(T_{10.8}) - L_{8.7}}{B_{8.7}(T_{10.8})}. \quad (2)$$

The tests applied are the following:

- Ice clouds are those with  $T_{10.8} < -30^{\circ}\text{C}$  or with  $A_{3.9} < 0.029$  (an empirical threshold).
- Liquid water clouds are indicated for pixels with 3.9  $\mu\text{m}$  albedo greater than a second threshold AND when the 3.9  $\mu\text{m}$  albedo is greater than a background 3.9  $\mu\text{m}$  albedo (determined using the 3.9  $\mu\text{m}$  albedo corresponding to the warmest 10.8  $\mu\text{m}$  brightness temperature over the past ten days). The second threshold differs over land and ocean: over ocean, liquid water clouds are indicated if  $A_{3.9} > 0.18$ ; over land, liquid water clouds are indicated if  $A_{3.9} > 0.21$  (both empirically determined). In addition, over land  $A_{8.7}$  observations are used to eliminate bright desert; clouds are indicated only if  $A_{8.7} < 0.067$  (again, empirically determined).
- Clear sky is indicated if both of the above tests fail.

Figure 2 shows an example.

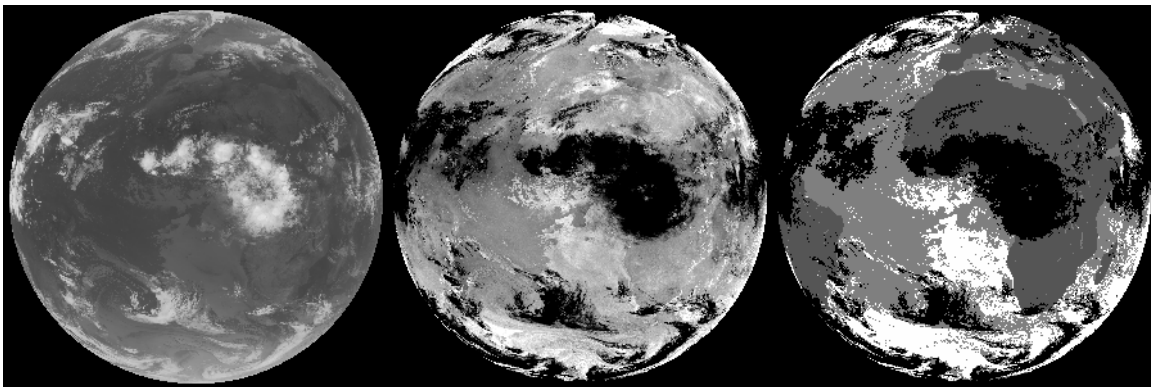


**Figure 2.**  $T_{10.8}$  (left);  $A_{3.9}$  (center); nocturnal cloud mask (right, black = cirrus, white=liquid water cloud, gray = no cloud). Note that the 10-day background test was not applied in this example.

The albedo and brightness temperature background (ALB/BTB) database contains the 3.9  $\mu\text{m}$  albedo and 10.8  $\mu\text{m}$  brightness temperature data observed over each Meteosat-8 pixel each day for the previous 10-day period. The data base is updated every hour. Thus, for each pixel the

database contains 10 entries for the historical 10-day record. When new data are processed, each database is updated with current 3.9  $\mu\text{m}$  albedo and 10.8  $\mu\text{m}$  brightness temperature values for each Meteosat-8 pixel location. The current 3.9  $\mu\text{m}$  albedo and 10.8  $\mu\text{m}$  brightness temperature values are used to update the ALB/BTB database by removing the oldest values and then shift all remaining ALB/BTB values by one day. This process assumes that there is no change in the image-to-image navigation of the Meteosat-8 data.

### 2.3. Daytime Cirrus

This daytime cirrus test for Meteosat-8 data utilizes three reflective channels, 0.6  $\mu\text{m}$ , 0.8  $\mu\text{m}$ , and 1.6  $\mu\text{m}$ . The measured radiances ( $L_i$ ) are converted to albedos (0 to 1) by dividing the radiances by the solar irradiance ( $S_i$ ) and by the cosine of the solar zenith angle, then multiplying by  $\pi$ :

$$A_i = \frac{\pi L_i}{S_i \cos(\zeta)} \tag{3}$$

If one constructs an RGB (red, green, blue) image from the albedos at these three wavelengths such that red is 1.6  $\mu\text{m}$ , green is 0.8  $\mu\text{m}$ , and blue is 0.6  $\mu\text{m}$ , one gets an image such as in Fig. 2. Liquid water clouds are highly reflective at all three wavelengths and, thus, appear white. Ice clouds (and snow on the ground) are highly reflective at 0.6 and 0.8  $\mu\text{m}$ , but poorly reflective at 1.6  $\mu\text{m}$ ; they therefore appear cyan (green + blue) in color.

The algorithm uses the three albedos as three dimensions (x, y, z) in the color cube (R, G, B). The pixels in the cyan portion of the color cube are identified as cirrus.

Pixels over snow-covered ground must be excluded from this calculation. Very thin cirrus clouds are often not “cyan” enough to be detected by this method. There can be false positives near the terminator.

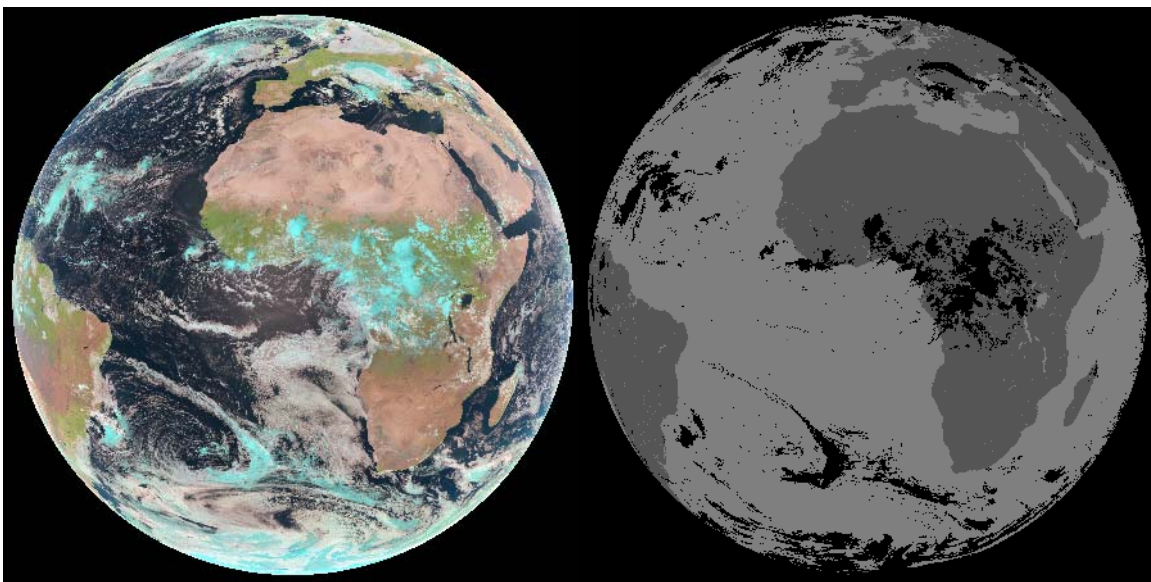


**Figure 3.** MSG tri-spectral image (left, R=1.6  $\mu\text{m}$ , G=0.8  $\mu\text{m}$ , B=0.6 $\mu\text{m}$ ); daytime cirrus cloud mask (right).

## 2.4. Nocturnal Thin Cirrus

The nocturnal thin cirrus test for Meteosat-8 data uses the albedo at  $3.9 \mu\text{m}$ , which is calculated from measured radiances at  $3.9 \mu\text{m}$  and  $10.8 \mu\text{m}$  (Kidder et al. 2000; Kidder 2002). Radiation from below the cloud leaks through thin cirrus, which results in a negative albedo. Nothing else results in a negative  $3.9 \mu\text{m}$  albedo, so this is a very sensitive test for thin cirrus at night. The technique does not work during daylight hours due to contamination of the  $3.9 \mu\text{m}$  observations by solar radiation. (See the black areas in the right hand portion of Fig. 2)

## 2.5. Precipitating Clouds

The precipitating cloud test for Meteosat-8 data uses the brightness temperature difference between the  $6.2 \mu\text{m}$  water vapor channel and the  $10.8 \mu\text{m}$  window infrared channel to detect high, thick clouds, which are likely to be precipitating.

At  $6.2 \mu\text{m}$  the atmosphere is opaque due to water vapor absorption. Low clouds are not sensed at  $6.2 \mu\text{m}$ ; only deep clouds penetrate the water vapor to be sensed at both  $6.2$  and  $10.8 \mu\text{m}$ , and when this happens the brightness temperature difference at these two wavelengths becomes small. When  $T_{10.8} - T_{6.2} < 11 \text{ K}$  (an empirically determined threshold), the pixel is flagged as precipitating cloud. This test is valid both day and night when the needed Meteosat-8 data exist (Fig. 4).

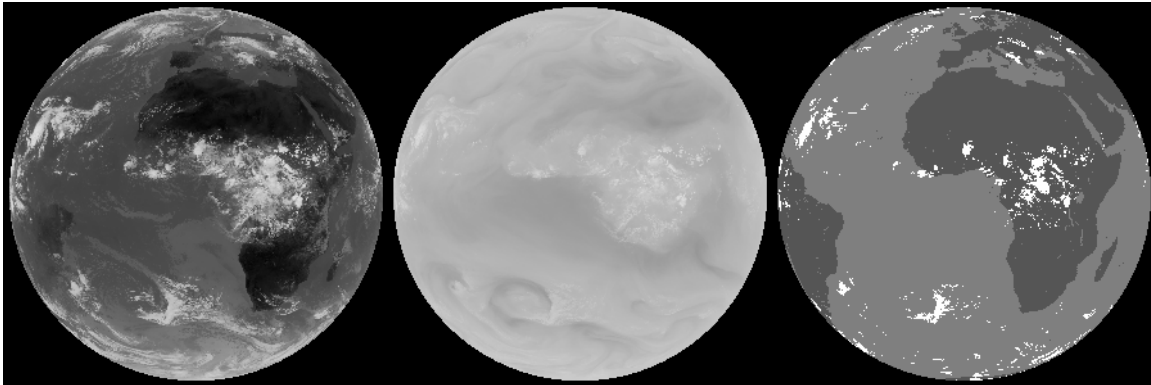


Figure 4.  $T_{10.8}$  (left);  $T_{6.2}$  (center); precipitating clouds (right).

## 2.6. Multi-Channel Skin Temperature

The Multi-Channel Satellite Skin Temperature Procedure for Meteosat-8 data employs two channels ( $10.8 \mu\text{m}$  and  $12.0 \mu\text{m}$ ) to determine the surface skin temperature. The classic “split window” technique of McMillin and Crosby (1984) is used. Both  $10.8$  and  $12.0 \mu\text{m}$  radiances are affected by water vapor in the column between the surface and the satellite, but  $10.8 \mu\text{m}$  is less affected than  $12 \mu\text{m}$ . The difference between the brightness temperatures at  $10.8$  and  $12 \mu\text{m}$  can be used to correct the  $10.8 \mu\text{m}$  brightness temperature for water vapor absorption to yield an estimate of the skin temperature, that is, the brightness temperature which would be observed if there were no water vapor in the atmosphere. A very similar technique has been used for many years to retrieve sea surface temperature from Advanced Very High Resolution Radiometer (AVHRR) data on the NOAA (polar orbiting) satellites (Strong and McClain 1984).

Note that the retrieved temperature is the skin temperature (the temperature of the surface itself), not the air temperature (the temperature measured in a standard weather instrument shelter approximately 2 m above the surface).

This procedure applies to clear-sky pixels only (although in cloudy areas it provides an estimate of cloud-top temperature).

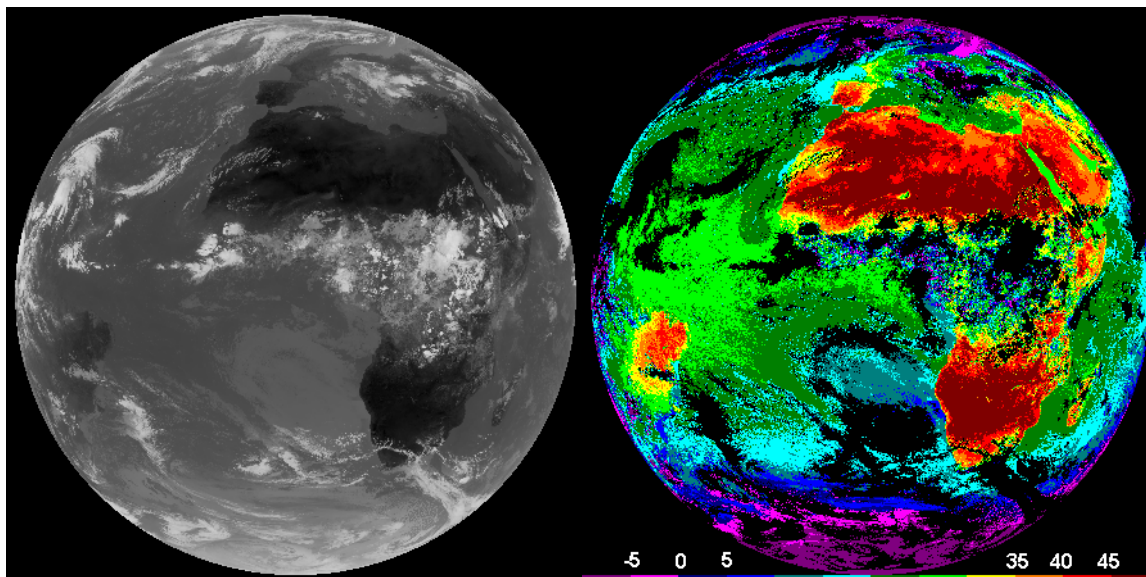


Figure 5.  $T_{10.8}$  (left); skin temperature ( $^{\circ}\text{C}$ , right), black areas are cloudy (see Fig. 1).

### 3. SUMMARY AND CONCLUSIONS

We have developed six algorithms utilizing Meteosat Second Generation data for implementation at AFWA: Cloud Mask, Nocturnal Cloud Mask, Daytime Cirrus, Nocturnal Thin Cirrus, Precipitating Clouds, and Multi-Channel Skin Temperature. The algorithms seem to work well, but they would all benefit from a more thorough validation study.

*Acknowledgement.* This research is supported by the DoD Center for Geosciences/Atmospheric Research at Colorado State University under the Cooperative Agreement (#DAAL01-98-2-0078) with the Army Research Laboratory.

### REFERENCES

- Kidder, S. Q., 2002: A measurement of the albedo of thick cirrus clouds at  $3.9\ \mu\text{m}$ . *Geophysical Research Letters*, Vol. 29, No. 9, 10.1029/2001GL014041, pp. 9–1 to 9–3.
- Kidder, S. Q., D. W. Hillger, A. J. Mostek, and K. J. Schrab, 2000: Two simple GOES Imager products for improved weather analysis and forecasting. *National Weather Digest*, **24**, 25–30.
- McMillin, L. M., and D. S. Crosby, 1984: Theory and validation of the multiple window sea surface temperature. *Journal of Geophysical Research*, **89**, 3655–3661.
- Schiffer, R. A., and W. B. Rossow, 1983: The International Satellite Cloud Climatology Project (ISCCP): The first project of the World Climate Research Programme. *Bulletin of the American Meteorological Society*, **64**, 779–784.
- Strong, A. E., and E. P. McClain, 1984: Improved ocean surface temperatures from space—comparisons with drifting buoys. *Bulletin of the American Meteorological Society*, **65**, 138–142.